Rare-Earth Metal Complexes Supported by Polydentate Phenoxy-Type Ligand Platforms: C-H Activation Reactivity and CO(2)/Epoxide Copolymerization Catalysis

Liye Qu, Thierry Roisnel, Marie Cordier, Dan Yuan, Yingming Yao, Bei Zhao, Evgueni Kirillov

Rare-Earth Metal Complexes Supported by Polydentate Phenoxy-Type Ligand Platforms: C–H Activation Reactivity and CO_2/Epoxide Copolymerization Catalysis

Liye Qu, [a,b] Thierry Roisnel,[c] Marie Cordier,[c] Dan Yuan, [a,*] Yingming Yao, [a,*] Bei Zhao, [a] Evgueni Kirillov [b,*]

[a] Key Laboratory of Organic Synthesis of Jiangsu Province, College of Chemistry, Chemical Engineering and Materials Science, Dushu Lake Campus, Soochow University, Suzhou 215123, People's Republic of China.

[b] Univ Rennes, CNRS, ISCR (Institut des Sciences Chimiques de Rennes), UMR 6226, F-35700 Rennes, France

[c] Centre de Crystallographie, Univ Rennes, CNRS, ISCR (Institut des Sciences Chimiques de Rennes), UMR 6226, F-35700 Rennes, France

ABSTRACT

Mono and dinuclear group 3 metal complexes incorporating polydentate bis(imino)phenoxy $\{N^2O\}^-$ and bis(amido)phenoxy $\{N^2O\}^{3-}$ ligands were synthesized by alkane elimination reactions from the tris(alkyl) $M(CH_2SiMe_3)_3(THF)_2$ and $M(CH_2C_6H_4\text{-}o\text{-}NMe_2)_3$ (M = Sc, Y) precursors. Complex **1a-Y** was used for the selective C–H activation of 2-phenylpyridine at

* Correspondence to Dan Yuan (yuandan@suda.edu.cn), Yingming Yao (yaoym@suda.edu.cn) and Evgueni Kirillov (evgueni.kirillov@univ-rennes1.fr).

the 2'-phenyl position affording the corresponding bis(aryl) product **3a-Y**, which was found to be reacted reluctantly with weak electrophiles (styrene, imines, hydrosilanes). The mechanism of formation of **3a-Y** was established by DFT calculations, which also corroborated high stability of the complex towards insertion of styrene, apparently stemming from the inability to form the corresponding adduct. Copolymerization of cyclohexene oxide and CO_2 promoted by **1a-Y** (0.1–0.5 mol%) was demonstrated to proceed under mild conditions (toluene, 70 °C, P_{CO_2} = 12 bar) giving polycarbonates with high efficiency (maximal TON of 460) and selectivity (97–99 % of carbonate units).

INTRODUCTION

Phenolate-based ligand platforms constitute strong and convenient alternative to cyclopentadienyl-type ligands for the modern coordination chemistry of the early transition metals, largely thanks to their remarkable tunability allowing diverse sterico-electronic variations.[1] In particular, these hard, electronegative π-donor ligands are attractive because they offer strong metal–oxygen bonds that are expected to stabilize complexes of highly oxophilic and electropositive metals (e.g. Group 3 metals).[2] Rare-earth metal alkyl complexes have shown great utility in many 100 % atom-economy catalytic reactions involving heteroatom-containing substrates, such as C–H activation/functionalization of anilines, anisoles, amines and heterocycles,[3,4] (co)polymerization of polar monomers (lactones, carbonates, epoxides)[5] and activation of CO_2.[6,7] As such, there is continued interest in designing better performing and more stable catalysts that also exhibit improved functional group tolerance.

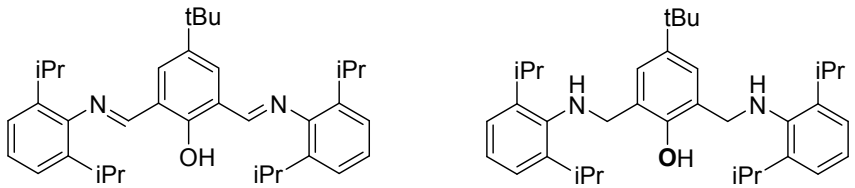

{N^2O}H (**1a-H**) {N^2O}H_3 (**1b-H_3**)

Scheme 1. Proligands 1a-H and 1b-H_3 Used in This Study.

Herein we report the synthesis and characterization of group 3 metal complexes supported by bulky multidentate bis(imino)phenolate and bis(anilino)phenolate ligand

systems (Scheme 1). The multidentate nature and high coordination abilities of these ligand platforms have initially been anticipated as beneficial for the preparation of dinuclear complexes or formation of dinuclear intermediates in catalytic processes. Special emphasis has been placed on (i) studies of the coordination chemistry of this ligand systems with scandium and yttrium, starting from tris(carbyl) precursors $LnR_3(THF)_x$, in order to achieve selective synthesis of the corresponding alkyl complexes; (ii) evaluation of potential of the titled alkyl complexes as precatalysts of C–H activation of 2-phenylpyridine and hydroarylation of styrene; (iii) stoichiometric reactions between alkyl complexes and 2-phenylpyridine mimicking the C–H activation step; (iv) evaluation of the efficacy of some complexes obtained during this study in copolymerization reactions of CO_2 with cyclohexene oxide (CHO).

RESULTS AND DISCUSSION

Synthesis of rare-earth metal complexes derived from proligands {N²O}H (1a-H) and {N²O}H₃ (1b-H₃). The proligands, bis(imino)phenol **1a-H** and bis(anilino)phenol **1b-H₃**, were prepared in good yields (29−60 %) using the protocols reported in the literature.[8] To study the coordination ability of these ligand platforms with group 3 metals (Sc, Y), σ–bond metathesis reactions between the corresponding proligands and metal tris(alkyls) $MR_3(THF)_2$ were investigated.

The reaction between **1a-H** and 1 equiv. of $Sc(CH_2SiMe_3)_3(THF)_2$ in C_6D_6 (Scheme 2), monitored by ^1H NMR spectroscopy, proceeded readily in the –25 to 25 °C range, completely consuming both reagents. However, the final ^1H NMR spectrum (Figure S4) showed two

series of resonances corresponding to two different products, mono-ligand bis(alkyl) **1a-Sc** and bis(ligand) mono-alkyl **1a-Sc'** in a respective ~1:0.3 ratio. This observation is in line with that by Piers *et al.* describing the preferential formation of a related bis(phenoxy-imino) scandium monoalkyl complex $\{\eta^2$-1-[CH=N-Ar]-2-O-3-*t*Bu-$C_6H_3\}_2ScCH_2SiMe_3$ (**I-Sc**) along with small amounts of the monoligand bis(alkyl) congener in the reaction between the equimolar amounts of the corresponding proligand and $Sc(CH_2SiMe_3)_3(THF)_2$.[9] In our case, the increased steric bulk of **{1a}**$^-$ contributes to a better stabilization of the monoligand bis(alkyl) species.

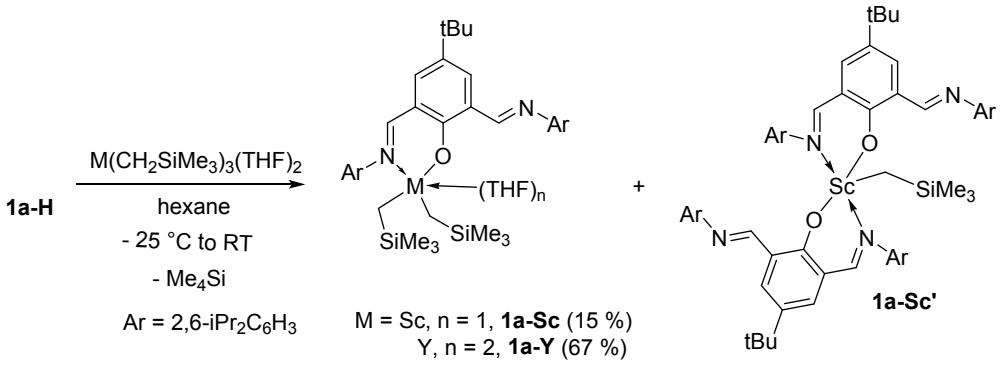

Scheme 2. Formation of Complexes 1a-M (M = Sc, Y) and 1a-Sc'.

More comprehensive NMR data ($^{13}C\{^1H\}$, ^1H–^1H COSY) were collected for this sample that allowed understanding the solution structures of both products and making assignments of characteristic resonances. For example, for **1a-Sc**, the key resonances in the room-temperature ^1H and $^{13}C\{^1H\}$ NMR spectra (Figures S4 and S7, respectively) include: (a) two broad signals from the two CH=N groups (δ_H 9.20, 8.16 ppm and δ_C 172.5, 158.6 ppm, respectively), (b) two broad signals from the C_6H_2 moiety (δ_H 9.02, 7.35 ppm and δ_C 131.6, 135.2 ppm, respectively), (c) one resonance for the ScCH_2 groups (δ_H –0.01 ppm and δ_C 40.4 ppm, respectively), (d) singlet resonance for the $SiMe_3$ groups (δ_H 0.08 ppm and δ_C

3.3 ppm, respectively). For **1a-Sc'**, similar key resonances include: (a) two sharp signals from the two pairs of the equivalent coordinated and non-coordinated CH=N groups (δ_H 7.93, 7.45 ppm and δ_C 172.5, 156.8 ppm, respectively), (b) two sharp signals from the non-equivalent protons of the two C_6H_2 moieties (δ_H 8.90, 7.19 ppm and δ_C 132.3, 134.8 ppm, respectively), (c) in the ^{1}H NMR spectrum, two doublets from the diastereotopic Sc*CHH* protons (δ_H 0.67 and –0.25 ppm) and a tiny singlet (δ_C 42.9 ppm) in the $^{13}C\{^1H\}$ NMR spectrum, (d) singlet resonance for the $SiMe_3$ groups (δ_H 0.00 ppm and δ_C –0.4 ppm, respectively). Upon increasing the temperature to 72 °C (Figure S5) both products appeared to be stable in solution, and no significant change in the pattern of signals was observed for **1a-Sc'**. On the other hand, for **1a-Sc**, substantial broadening was observed for the signals in the aromatic region, thus, suggesting the existence of some fluxional dynamic process probably related to the exchange between the coordinated and pending imino functions.[10] A small amount (15 % yield) of pure complex **1a-Sc** was isolated by recrystallization and characterized by X-ray crystallography (vide infra).

Similar NMR scale reaction between **1a-H** and 1 equiv. of $Y(CH_2SiMe_3)_3(THF)_2$ in C_6D_6 afforded **1a-Y** quantitatively as judged by ^{1}H NMR spectroscopy. Thus, the scaled-up synthesis was repeated allowing isolation of pure **1a-Y** in 67 % yield after recrystallization (Scheme 2). Complex **1a-Y** was characterized by ^{1}H and ^{13}C NMR spectroscopy and X-ray crystallography. For this compound, a complex fluxional behavior in solution was observed over a broad temperature range. For example, the room-temperature ^{1}H NMR spectrum of **1a-Y** (Figure S8) exhibited a series of broadened signals, only a few of them could be unequivocally assigned: very broad signals at δ_H 9.00–7.50 ppm from the C*H*=N and C_6H_2

groups, broad multiplet at δ_H 3.18 ppm from the C*H*$(CH_3)_2$ protons and singlets at δ_H 0.12 and −0.71 ppm from the Si(C*H*$_3)_3$ and C*H*$_2$ protons, respectively, of the Y−$CH_2Si(CH_3)_3$ groups. Upon lowering temperature to −40 °C **1a-Y** (Figure S9), the broad signals in the aromatic regions split into two pairs of broad singlets, while the resonance from the C*H*$_2$ protons in the high-field split into a series of three broad signals. Though, more detailed information about the solution structure of **1a-Y** could not be obtained, these observations are consistent with the existence of the same exchange processes as those depicted for **1a-Sc** and **I-Sc**.[9]

The molecular structures of **1a-Sc** (Figure S1) and **1a-Y** (Figure 1) are comparable to those of the penta-coordinate {η^2-1-[CH=N-Ar]-2-O-3-*t*Bu-C_6H_3}Y$(CH_2SiMe_3)_2$(THF) and six-coordinate {η^2-1-[CH=N-Ar]-2-O-3-*t*Bu-C_6H_3}Y$(CH_2SiMe_3)_2(THF)_2$ complexes, respectively, reported previously.[9] Thus, the respective distorted trigonal-bipyramidal and octahedral coordination environments around the metal centers are perfectly reproduced in the structures of **1a-Sc** and **1a-Y**. In **1a-Y**, the Y−C(carbyl) and Y−N(1) bond lengths (2.423(2), 2.438(2) and 2.5159(18) Å, respectively) are in the range of those observed in the two yttrium complexes (2.398–2.440 and 2.466–2.661 Å, respectively),[9] while the Y−O(1) distance (2.1994(15) Å) is only slightly longer (2.121–2.166 Å). In **1a-Sc**, the same bond lengths (2.2100(16), 2.2333(16), 2.0198(11) and 2.3502(13) Å, respectively) are shorter than those in the yttrium congener, which is in line with the decrease of the effective ionic radii of the Sc(3+) metal ion.[11]

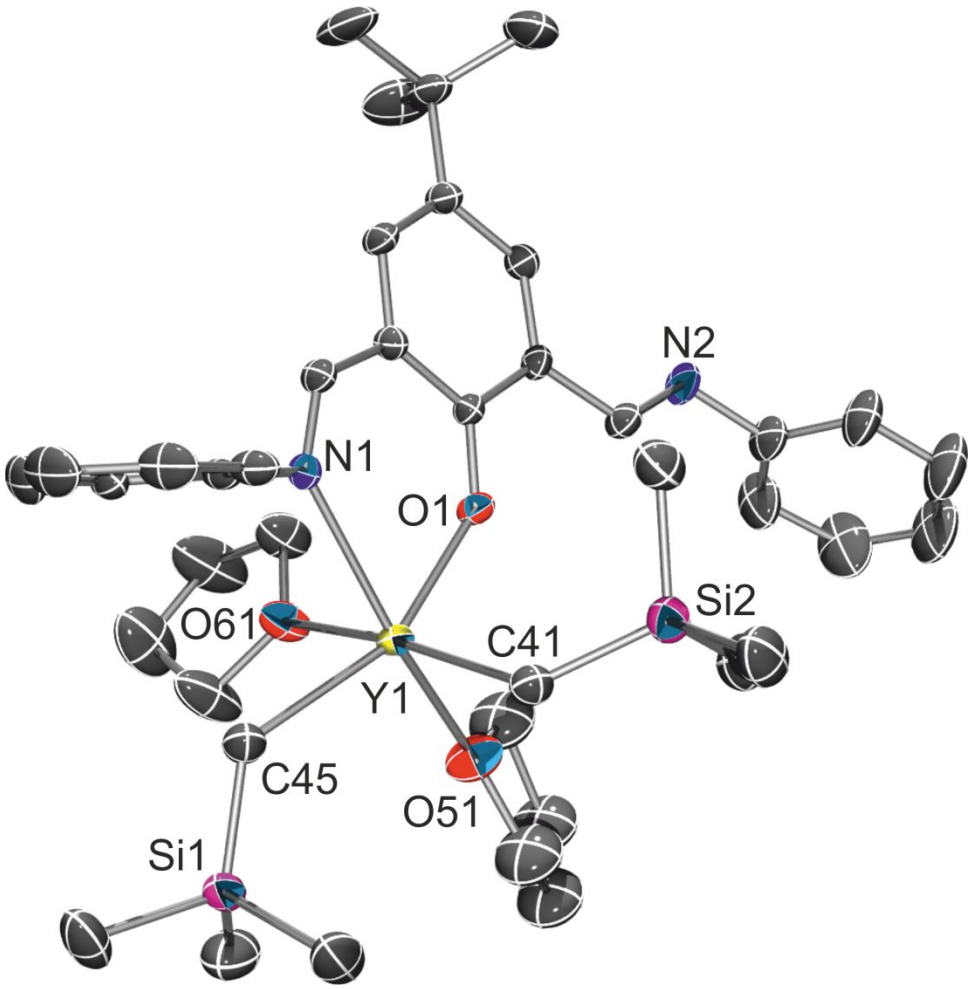

Figure 1. Molecular structure of $\{N^2O\}Y(CH_2SiMe_3)_2(THF)_2$ (**1a-Y**) (all hydrogen atoms and 2,6-iPr_2 groups are omitted for clarity; thermal ellipsoids drawn at the 50 % probability). Selected bond distances (Å) and angles (°): Y(1)–O(1), 2.1994(15); Y(1)–O(51), 2.3779(18); Y(1)–N(1), 2.5159(18); Y(1)–C(41), 2.423(2); Y(1)–C(45), 2.438(2); Y(1)–O(61), 2.4637(17); O(51)–Y(1)–N(1), 160.20(6); C(45)–Y(1)–O(61), 86.17(7); C(41)–Y(1)–O(61), 168.96(8).

In the attempts to synthesize dinuclear complexes, potentially incorporating two M-$(CH_2SiMe_3)_x$ groups united by one multifunctional $\{N^2O\}^-$ ligand scaffold, upon reacting **1a-H** with 2 equiv. of $M(CH_2SiMe_3)_3(THF)_2$ only the formation of **1a-M** together with the

unreacted tris(alkyl) precursor took place, as judged by ^{1}H NMR spectroscopic studies of the corresponding crude reaction mixtures.

In attempts to synthesize dinuclear complexes, in which two metal centers are linked by a single ligand platform, regular alkane elimination reactions of **1b-H$_3$** with the corresponding rare-earth metal precursors M(CH$_2$SiMe$_3$)$_3$(THF)$_2$ (M = Sc, Y) in the corresponding 1:2 ratio were studied. However, only alkyl group-free dinuclear bis(ligand) complexes **[1b-M]$_2$** were isolated (Scheme 3). For instance, monitoring by ^{1}H NMR spectroscopy of the reaction of **1b-H$_3$** with 2 equiv. of M(CH$_2$SiMe$_3$)$_3$(THF)$_2$ confirmed the quantitative formation of these products, while 1 equiv. of the tris(alkyl) precursor remained intact in each case. The larger scale syntheses of complexes **[1b-M]$_2$** were optimized by using equimolar amounts of the two reagents. Both compounds were found stable in benzene-d_6 or toluene-d_8 solutions at 60 °C for days.

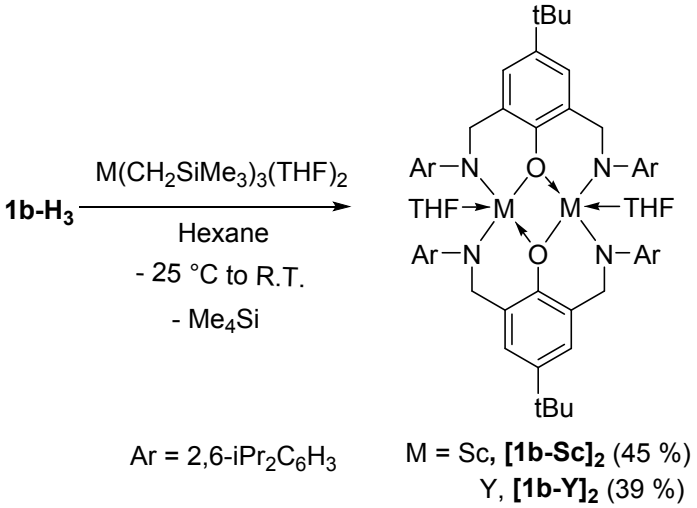

Scheme 3. Formation of Complexes [1b-M]$_2$.

Both complexes featured fluxional behavior in a broad range of temperatures, apparently associated with a restricted rotation of bulky bis(isopropyl)phenyl groups. The

room-temperature ^{1}H NMR spectra of **[1b-Sc]$_2$** and **[1b-Y]$_2$** (Figures S12 and S16, respectively) contained in each case a series of resonances consistent with the average C_2-symmetry of molecules. For **[1b-Sc]$_2$**, the four broadened characteristic signals from the two pairs of diastereotopic protons of the CH_2N groups were observed at δ_H 5.29, 4.06, 3.85 and 2.97 ppm in the ^{1}H NMR spectrum and the corresponding two resonances at δ_C 62.8 and 55.8 ppm in the ^{13}C NMR spectrum. The same groups in **[1b-Y]$_2$** afforded two well-resolved doublets δ_H 5.25 and 3.95 ppm ($^{2}J_{HH}$ = 14.6 Hz) and two resonances at δ_C 62.6 and 59.5 ppm at in the corresponding ^{1}H and ^{13}C{^{1}H} NMR spectra.

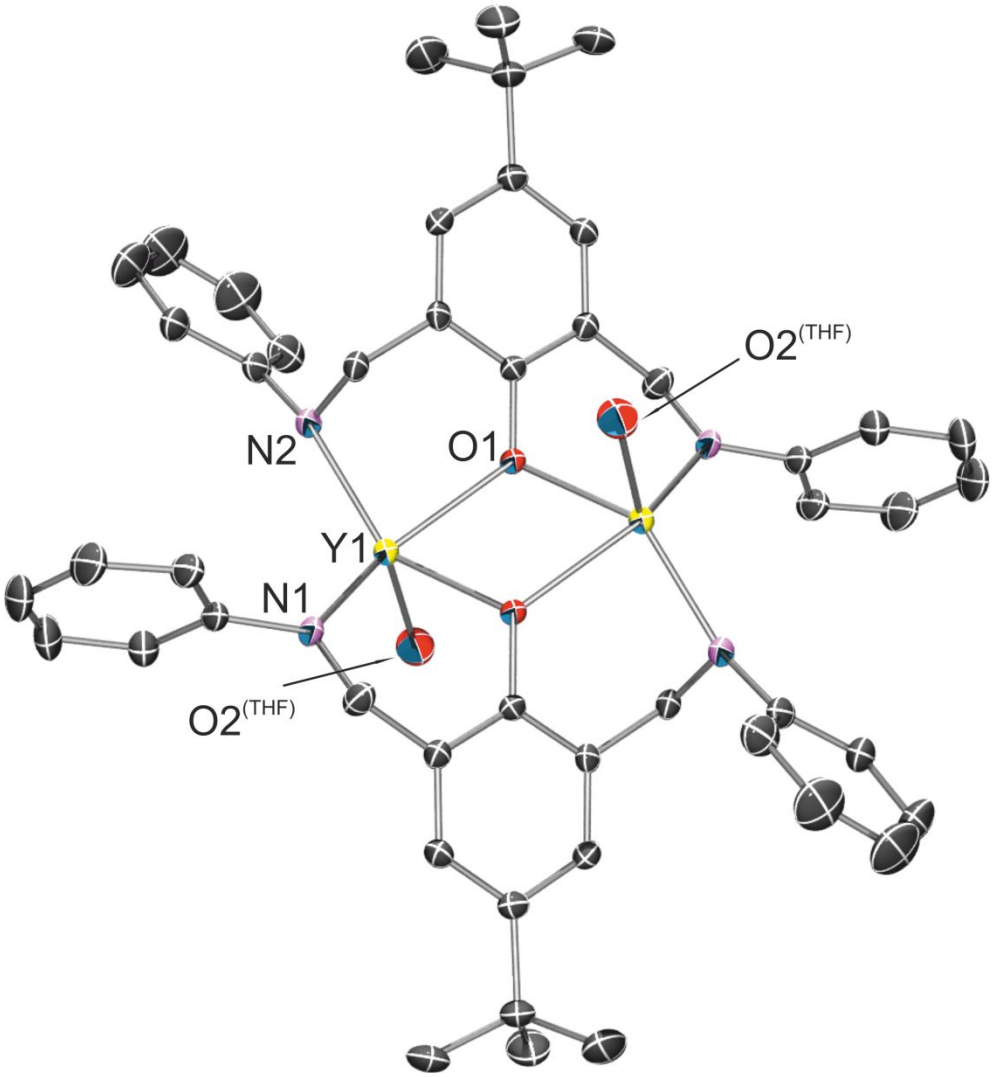

Figure 2. Molecular structure of **[1b-Y]$_2$** (all hydrogen atoms and *iPr* groups are omitted for

clarity; thermal ellipsoids drawn at the 50 % probability). Selected bond distances (Å) and angles (°): Y(1)–O(1), 2.278(4); Y(1)–O(2), 2.337(4); Y(1)–N(1), 2.212(5); Y(1)–N(2), 2.190(4); O(1)–Y(1)–N(1), 83.12(15); O(2)–Y(1)–N(2), 116.62(18); N(1)–Y(1)–N(2), 106.17(17).

The molecular structures of **[1b-Sc]$_2$** and [**1b-Y]$_2$** are depicted in Figure S3 and Figure 2, respectively. In unit cell of **[1b-Y]$_2$** contains three independent molecules featuring very similar geometrical parameters (bond lengths and angles) and overall organizations, and therefore the structural details of only one of them is discussed hereafter. Isostructural **[1b-Sc]$_2$** and **[1b-Y]$_2$** exhibit each the two five-coordinated metal atoms whose geometries are best described as distorted trigonal bipyramidal composed by two nitrogen and three oxygen atoms of the two $\{N^2O\}^{3-}$ ligands and one THF molecule. Thus, the M–O and M–N bonds (2.090(3)–2.143(3) and 2.006(3)–2.087(3) Å, respectively) with ligand in **[1b-Sc]$_2$** are shorter than those in the yttrium analogue (2.278(4)–2.337(4) and 2.190(4)–2.212(5) Å, respectively) by 0.14–0.24 Å, in line with the larger ionic radius of yttrium.[11] Also, the intermetallic M…M distances in these dinuclear molecules (3.4832(12) and 3.9228(16) Å, respectively) are not exceptional[12] and are larger than the sum of the corresponding ionic radii (1.490 and 1.800 Å, respectively).[11]

Stoichiometric and catalytic studies on the reactivity of bis(alkyl) complex 1a-Y with 2-phenylpyridine. The C–H bond addition of heterocycles (hydroarylation) to alkenes or imines, catalyzed by alkyl complexes of group 3 metals, is known to follow a multi-step mechanism[3,4] involving the *ortho*-C(sp^2)–H activation reaction of an aromatic molecule

affording aryl intermediate, followed by insertion of the C=C or C=N bond into the M–aryl bond. Stoichiometric reactivity of group 3 metals alkyls with 2-phenylpyridine has also been the subject of several studies. For example, the formation of different C–H bond activation products incorporating η^2-*N*,*C*-6-phenylpyridyl,[13] η^2-*N*,*C*-2'-phenylpyridyl[13a,14,15] or the 2-phenypyridine-derived biheterocyclic[13a,b,c,14b] ligands have been reported. In particular, Diaconescu *et al.*[13a] observed in the corresponding yttrium and lutetium complexes the slow rearrangement process for the 2-phenylpyridine ligand from the η^2-*N*,*C*-6-phenylpyridyl (three-membered-ring metallocycle) to the more stable η^2-*N*,*C*-2'-phenylpyridyl (five-membered-ring metallocycle) coordination mode.

In order to assess the potential of bis(alkyl) complex **1a-Y** in C(sp^2)–H activation/hydroarylation reactions, its reactivity with 2-phenylpyridine was preliminary studied. Monitoring by ^{1}H NMR spectroscopy of the reaction between equimolar amounts **1a-Y** and 2-phenylpyridine in C_6D_6 at room temperature (Figure S18) showed slow disappearance of the signal at δ_H –0.71 ppm from the CH_2 protons of the Y–$(CH_2Si(CH_3)_3)_2$ groups, and the appearance of a new signal at δ_H –0.28 ppm. The latter apparently belongs to the Y–$CH_2Si(CH_3)_3$ group from a new mixed mono-alkyl/aryl species resulted from C–H activation reaction of 2-phenylpyridine (Scheme 4). Unfortunately, all attempts to isolate and authenticate this putative product failed.

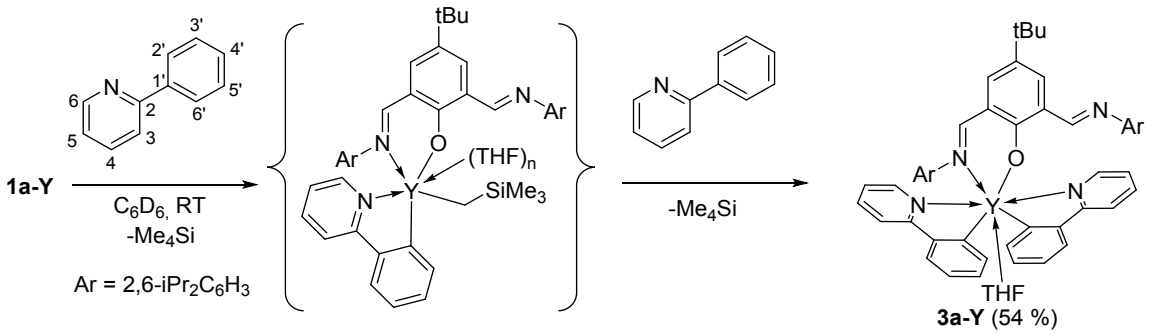

Scheme 4. Formation of Complex 3a-Y From 1a-Y and 2-Phenylpyridine.

Similar reaction between **1a-Y** and 2 equiv. of 2-phenylpyridine after 16 h resulted in a complete consumption of **1a-Y** and in formation of complex **3a-Y** (Scheme 4). Complex **3a-Y** was re-prepared on a larger scale and isolated in 54 % as dark green crystals. The nature of the compound was authenticated by ^{1}H and ^{13}C NMR spectroscopy and X-ray crystallography. In particular, the room-temperature ^{1}H NMR spectrum of **3a-Y** was slightly broadened due to fluxional behavior possibly arising from ligand rearrangement. The ^{1}H and ^{13}C{^{1}H} NMR spectra (Figures S19 and S22) exhibited a single set of resonances, consistent with an average C_s-symmetric species on the NMR time scale, in which the two η^2-*N*,C-2'-phenylpyridyl fragments are equivalent. In particular, the ^{13}C{^{1}H} NMR spectrum of **3a-Y** (Figure S22) contained only one characteristic doublet (δ_C 190.8 ppm, $^{1}J_{Y-C}$ = 41.6 Hz)[14] for the two Y-*C* carbon atoms of the two 2-phenyl-pyridyl groups. Upon lowering temperature to −33 °C (Figure S20) the very broad signal from the C*H*=N groups split into two single resonances at δ_H of 9.57 to 8.76 ppm, while for many other signals the pattern did not change significantly. At higher temperature (80 °C), a new series of resonances appeared after 1 h suggesting gradual decomposition of the compound affording unidentified products.

The five-membered-ring metallocyclic ring of complex **3a-Y** exhibiting

η^2-*N*,*C*-2'-phenylpyridyl coordination of the ligand parallels previous results obtained by different groups.[13a,14,15] It should be also mentioned that the existence of a possible isomerization process in solution similar to that described by Diaconsescu *et al.*[13a] and consisting in our case in the change of the mode of coordination of the 2-phenyl-pyridyl ligand in **3a-Y** from η^2-*N*,*C*-2'-phenylpyridyl to η^2-*N*,*C*-6-phenylpyridyl type could not be unequivocally established by our experimental techniques.

The molecular structure of **3a-Y** (Figure 3) revealed the yttrium atom in a seven-coordinated environment provided with the oxygen atom and the nitrogen atom of the $\{N^2O\}^-$ ligand, the two carbon and two nitrogen atoms of the two monoanionic phenyl-pyridine ligands and the oxygen atom of the coordinated THF molecule. In **3a-Y**, the Y–O and Y–N distances (2.2225(16) and 2.519(2) Å) for the coordinated phenoxy-imino ligand are very close to those in the parent **1a-Y**. The Y–C(aryl) and Y–N(aryl) bond lengths (2.502(2), 2.505(2) and 2.504(2), 2.583(2) Å, respectively) in the seven-coordinated **3a-Y** are longer than those (2.449–2.480 and 2.453–2.506 Å, respectively) observed for the previously reported five- and six-coordinated yttrium complexes bearing the same η^2-*N*,*C*-2'-phenylpyridyl ligands.[13,14,15]

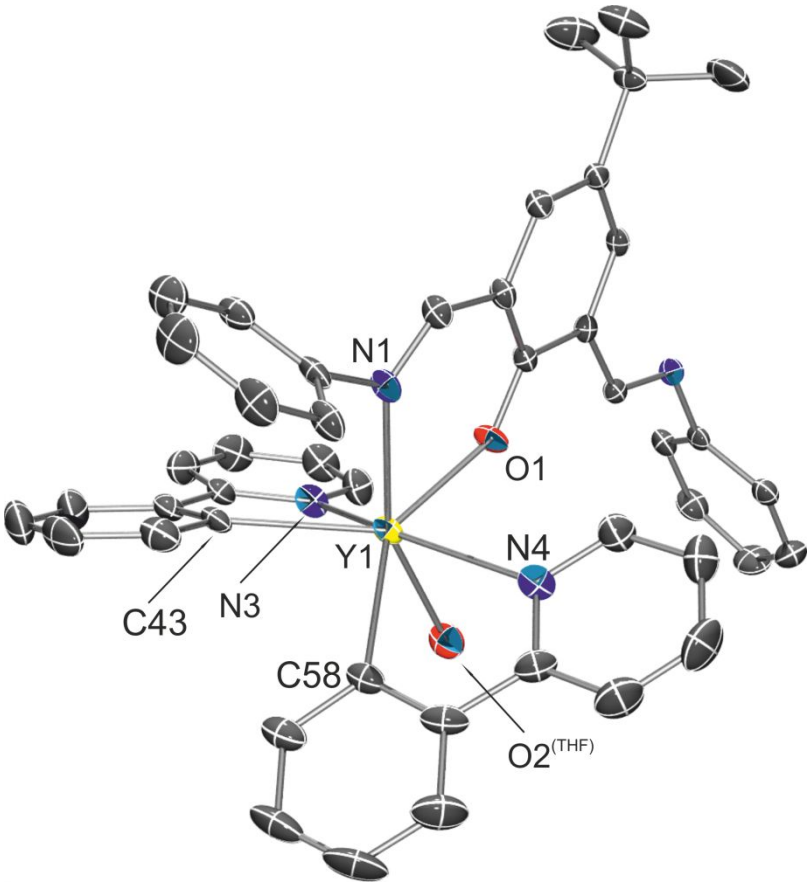

Figure 3. Molecular structure of **3a-Y** (all hydrogen atoms and iPr groups are omitted for clarity; thermal ellipsoids drawn at the 50 % probability). Selected bond distances (Å) and angles (°): Y(1)–O(1), 2.2225(16); Y(1)–O(2), 2.4167(17); Y(1)–C(47), 2.502(2); Y(1)–C(58), 2.505(2); Y(1)–N(1), 2.519(2); Y(1)–N(3), 2.504(2); Y(1)–N(4), 2.583(2); O(1)–Y(1)–O(2), 85.46(6); O(1)–Y(1)–C(47), 132.75(7); O(1)–Y(1)–N(3), 82.26(7); N(4)–Y(1)–C(58), 66.40(8); N(3)–Y(1)–C(47), 66.73(7).

In order to evaluate the feasibility of the alkylation of styrene with 2-phenylpyridine in the presence of **1a-Y**, stoichiometric reactions between complex **3a-Y** and styrene were monitored by ^{1}H NMR spectroscopy. Unfortunately, no reaction was observed in the temperature range 25–60 °C with 1–10 equiv. of styrene. Further increasing of the

temperature to 100 °C resulted only in decomposition of **3a-Y**, with no detectable insertion of styrene into the Y–(pyridine-2'-ylbenzene) bond.

To gain a better insight into the mechanism of C–H activation of 2-phenylpyridine with the bis(alkyl) complex **1a-Y**, DFT computations were conducted (Scheme S2). The objectives of these non-exhaustive computations were to assess and compare the energy profiles for several possible concurrent processes: a) C–H activation reaction of 2-phenyl-pyridine at the 2'-phenyl position resulting in formation of **3a-Y** (**E**$(THF)_x$, where x = 1), b) an alternative C–H activation reaction of 2-phenyl-pyridine at the 6-pyridyl position affording the corresponding isomeric **E'**$(THF)_x$ product. Also, the reactivity of the two products of the *ortho*-metallation reactions, bis(aryl) complexes **E**$(THF)_x$ and **E'**$(THF)_x$ (x = 0, 1), towards styrene was probed computationally, and the role of the presence of coordinated THF molecules on the stability and reactivity of key intermediates was assessed. The computational results were found to be in agreement with the experimental reactivity trends (see SI for details and discussion).

The catalytic performance of **1a-Y**, in combination with $B(C_6F_5)_3$,[4a] $[Ph_3C]^+[B(C_6F_5)_4]^-$ [4b] or nBu_2NH [4g] as cocatalysts, was briefly explored in hydroarylation of styrene with 2-phenylpyridine. Each reaction was carried out in a Teflon-valved sealed NMR tube, and the progress of reaction was monitored by ^1H NMR spectroscopy.

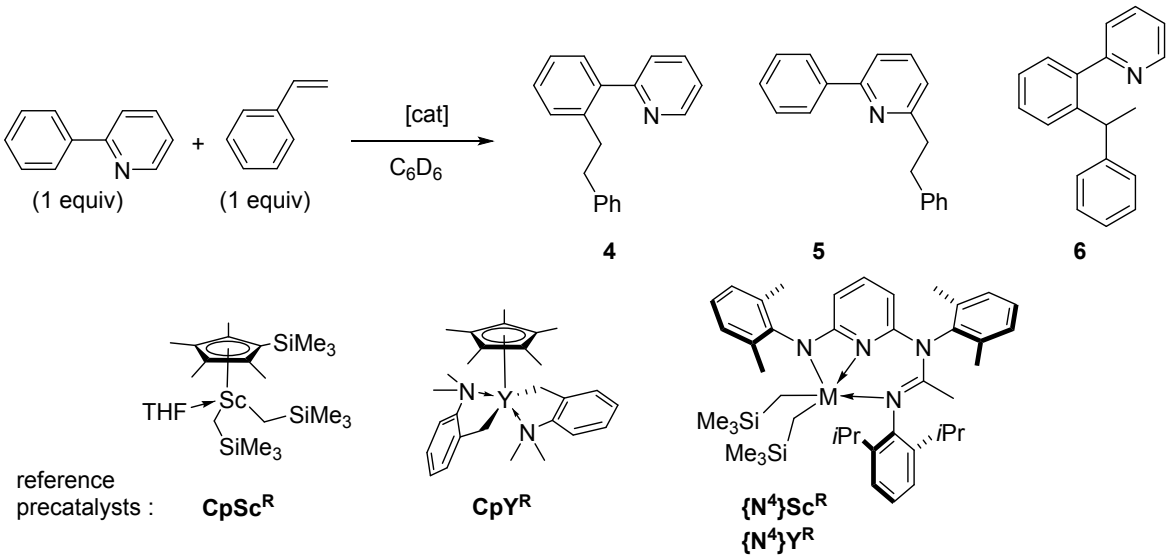

Scheme 5. Hydroarylation of Styrene With 2-Phenylpyridine.

For benchmarking purposes, the catalytic performance of several bis(alkyl) complexes of scandium and yttrium **CpM^R** [4b] and **{N^4}M^R** [16] (Scheme 5) as reference catalyst precursors, was explored under our experimental conditions (70–100 °C, C_6D_6; Table S2). Among the most successful results, the combination (10 mol%) of **CpSc^R** with $B(C_6F_5)_3$ afforded selectively 2-phenyl-6-(2-phenylethyl)pyridine (**5**) with 53 % conversion after 96 h at 70 °C. Also, the high selectivity in alkylation of 2-phenylpyridine with styrene was achieved with the binary system **{N^4}M^R**/$[Ph_3C]^+[B(C_6F_5)_4]^-$ at 100 °C (Table S2, entries 8–10). The catalytic system of **CpY^R**/ $[Ph_3C]^+[B(C_6F_5)_4]^-$ (2.5 mol%) appeared to be active in *ortho*-alkylation of anisole with styrene affording quantitatively 1-MeO-2-(2-phenylethyl)benzene after 24 h, which fits well with the result of Hou *et al.* reported to provide 94 % yield under the same conditions.[4b]

Under the same or modified conditions, poor catalytic results were achieved using complex **1a-Y** as precatalyst (Table S4). For example, only the combination

1a-Y/$[Ph_3C]^+[B(C_6F_5)_4]^-$ afforded small amounts (6 %) of **5** at 100 °C (Table S4, entries 4 and 5). Given the molecules of **1a-Y** and **3a-Y** both contain coordinated THF molecules, the absence of activity in catalysis, and particularly, reactivity towards styrene, could be attributed to a strong coordination of THF ligand, thus, impeding its displacement by such a poor donor as styrene. In order to address this issue, several catalytic experiments were conducted in the presence of substoichiometric or stoichiometric amounts of LiCl or $AlMe_3$ as possible scavengers of THF. However, only in one experiment using $AlMe_3$ (20 mol%) formation of only a small amount of 2-(2-(1-phenylethyl)-phenyl)-pyridine (**6**, 5 %) was observed (Table S4, entry 8). No visible formation of products were detected when other electrophilic substrates (e.g. *N*-R-1-phenyl-methanimine (R = Ph, *i*Pr), $PhSiH_3$, Et_3SiH) were used in the place of styrene.

Studies on copolymerization of CO_2 with cyclohexene oxide. The mononuclear bis(alkyl) **1a-Y** and dinuclear alkyl-free complexes **[1b-M]$_2$** were then tested as initiators of copolymerization of CO_2 with cyclohexene oxide (Scheme 6). For benchmarking purposes, first the copolymerization reactions initiated by {BDI}Zn(N(SiMe$_3$)$_2$)[17] was studied at 70 °C and 12 bar CO_2 pressure (Table 1, entry 1) affording 10 % conversion of monomer after 64 h. The low activity compared with the result reported by Coates *et al.*,[17] which gave 44 % conversion at 50 °C after 2 h, is apparently due to the addition of solvent (toluene), as the copolymerization rate law features a first order dependence on monomer concentration.[18] To our delight, using complex **1a-Y** as catalyst under the same conditions gave 95 % conversion and 97 % selectivity for polymers (entry 2). The yields remained almost unchanged when the loading of **1a-Y** decreased from 0.5 to 0.2 mol% (entries 3 and 5). Decreasing the concentration of **1a-Y** to 0.1 mol % led to a significantly lower conversion of 57 % (entry 12), suggesting high sensitivity of the initiating system to the presence of impurities. Similar observation on the decrease of the polymer conversion upon reducing the catalyst loading to 0.1 mol% was reported for the series of β-diimine bis(alkyl) yttrium complexes.[7b]

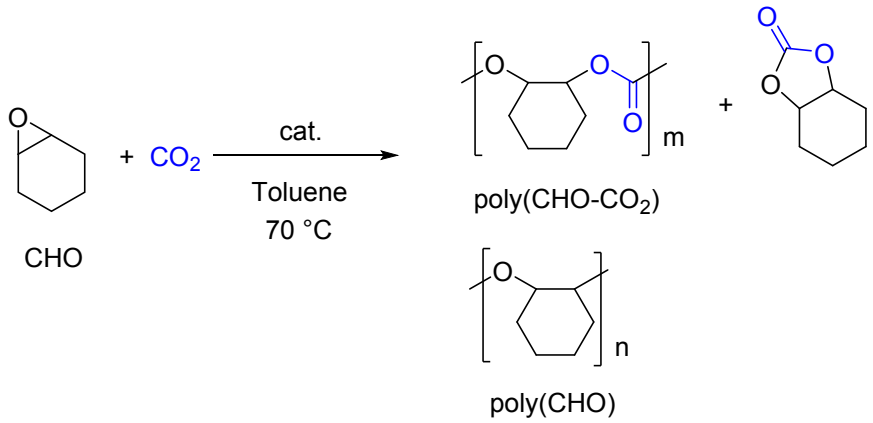

Scheme 6. Copolymerization of Cyclohexene Oxide (CHO) and CO_2 Catalyzed by Complex 1a-Y.

Table 1. Copolymerization of CO_2 With CHO Catalyzed by Complex 1a-Y.[a]

Entry	Initiator (%)	T (°C)	Time (h) [b]	Conversion (%) [c]	Polymer[c]	Carbonate units[c]	$M_{n,GPC}$ ($M_{n,calc}$) 10^3 g·mol^{-1} [e]	Đ [e]
1	**BDIZnNTMS$_2$** (0.5)	70	64	10	89	99	-	-
2	**1a-Y** (0.5)	70	64	95	97	99	8.1 (27.0)	1.49
3	**1a-Y** (0.5)	70	18	95	97	99	2.4 (27.0)	1.92
4	**1a-Y** (0.2)	25	18	<1	-	-	-	-
5	**1a-Y** (0.2)	70	18	95	>99	99	7.9 (67.5)	1.99
6	**1a-Y** (0.2)	50	18	86	>99	99	10.6 (61.1)	3.30
7	**1a-Y** (0.2)	70	1	22	>99	99	5.0 (15.6)	2.65
8	**1a-Y** (0.2)	70	2	41	>99	99	5.4 (29.1)	2.10
9	**1a-Y** (0.2)	70	3	75	>99	99	6.1 (56.9)	1.78
10	**1a-Y** (0.2)	70	4	84	>99	99	5.8 (59.7)	1.90
11	**1a-Y** (0.2)	70	5	92	>99	99	6.6 (65.4)	1.89
12	**1a-Y** (0.1)	70	18	57	>99	98	12.4 (80.9)	7.75
13[f]	**1a-Y** (0.2)	70	18	60	99	99	10.9 (42.6)	8.30
14	**1a-Y**/$ZnEt_2$ (0.2)	70	18	9	99	99	-	-
15	**1a-Y**/$MgBu_2$ (0.2)	70	18	8	99	99	-	-
16	**1a-Y**/$AlMe_3$ (0.2)	70	18	14	95	99	4.1 (10.0)	3.38
17	**[1b-Sc]$_2$** (0.2)	70	18	14	>99	<1	2.2 (6.86)	2.92
18	**[1b-Y]$_2$** (0.2)	70	18	31	>99	<1	3.0 (15.2)	1.72

[a] Reaction conditions: solvent = toluene (1.0 mL); $[CHO]_0$ = 4.95 mol·L^{-1}; 70 ºC; P_{CO2} = 12 bar; $[CO_2]/[CHO]$ = 5.3; n.o. = not observed. [b] Reaction times were not necessarily optimized. [c] Conversion of product and selectivity were determined by ^{1}H NMR spectroscopy. [d] Determined by DSC. [e] Determined by GPC; Đ = M_w/M_n. [f] Experiment conducted in the presence of cyclohexane-1,2-diol (2 equiv. *vs* **1a-Y**).

The reaction temperature appeared to have a significant influence on the copolymerization activity. While the experiment conducted at room temperature resulted in no polymer formation (entry 4), at 50 °C, a conversion of 86 % was observed after 18 h (entry 6). The highest conversion of 92 %, using 500 equiv. of CHO (TON of 460), achieved after 5 h at 70 °C (entry 11). Compared to the reported bis(alkyl) yttrium complex supported by β-diiminate ligand giving TON of 300 at 130 ºC and 15 bar CO_2 pressure,[7b] **1a-Y** proved to be one of the most efficient mononuclear rare-earth metal-based catalyst for polycarbonate synthesis. However, the activity of **1a-Y** is still lower than those reported for most highly active catalysts systems,[19] such as Lu's bifunctional Co(III)-salen catalysts,[19a] Rieger's very active di-zinc macrocyclic systems,[19b] La/Zn heteropolymetallic catalysts of Okuda and Mashima,[19c] Nozaki's porphyrin-based catalysts[19d] and Williams's heterobimetallic Mg/Co complexes[19e].

In order to determine orders on CHO and catalyst, a series of kinetic studies was undertaken. Kinetic monitoring of copolymerization under regular conditions (Figure S25) did not exhibit a significant induction period, regardless the catalyst concentration, suggesting rapid initiation with Y– CH_2SiMe_3 groups. The latter fact was corroborated by MALDI-ToF spectroscopy (Figure S31) demonstrating the presence of CH_2SiMe_3 end-groups in the low molecular weight polycarbonate sample (Table 1, entry 9). The first-order dependence both on the CHO concentration (Figure 4) and on the concentration of catalyst (Figure S26) was

determined from the corresponding linear plots, indicating a mononuclear pathway.[18,20]

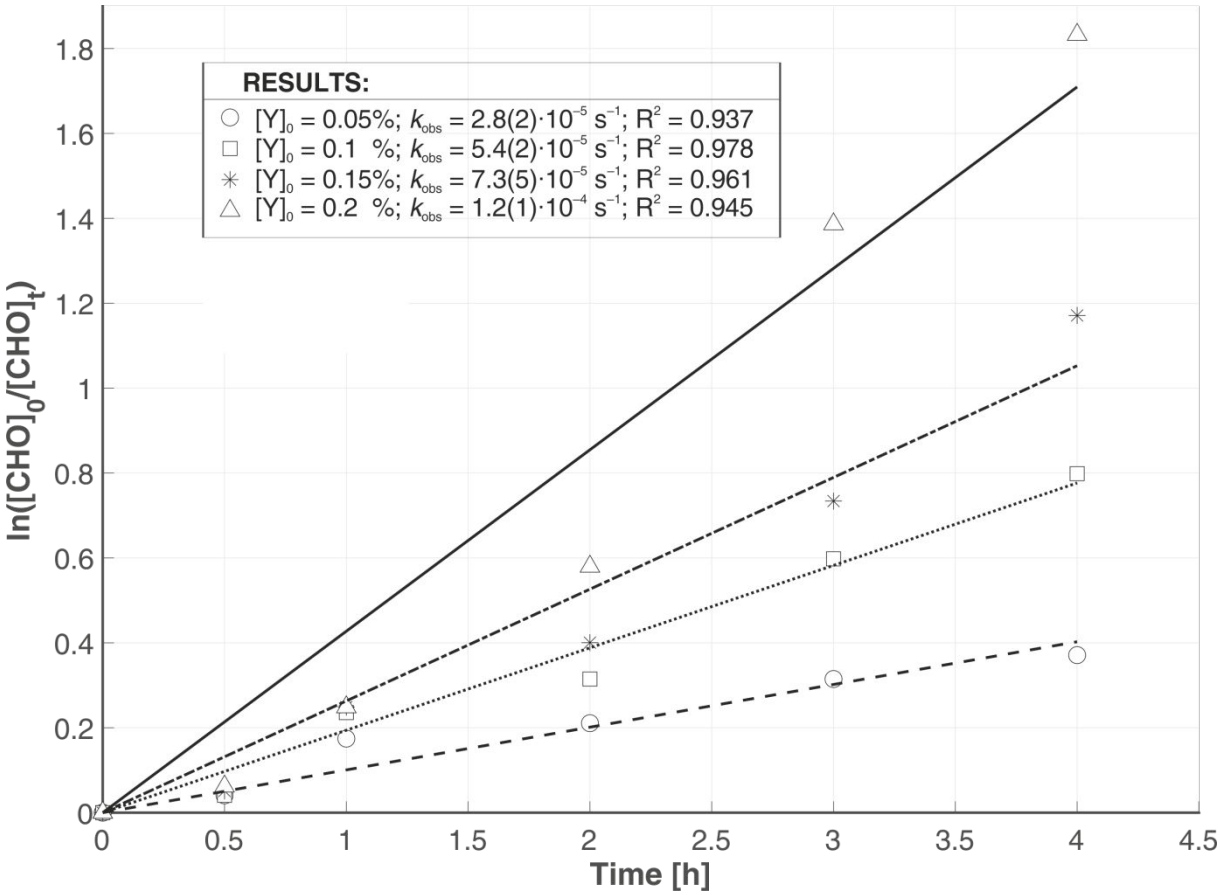

Figure 4. Plot of $\ln([CHO]_0/[CHO]_t)$ as a function of time for the copolymerization of CO_2 with CHO catalyzed by complex **1a-Y** (0.05–0.2 mol%); conditions: toluene, P_{CO2} = 12 bar, 70 °C, $[CHO]_0 = 4.95\ mol \cdot L^{-1}$.

Predominantly alternating polycarbonates rather than cyclic carbonates were isolated in all experiments involving **1a-Y** (e.g. entries 6 and 7), regardless of the reaction temperature. The polycarbonate polymers produced were essentially atactic as judged from the corresponding $^{13}C\{^1H\}$ NMR data (Figure S29) obtained for the sample of low M_n of 8,100 $g \cdot mol^{-1}$ (entry 2). Thus, in the carbonyl region, the intensity pattern of the corresponding key resonances at δ_C 153.8 ppm from the isotactic tetrads ([*mmm*], [*mmr*]) and at δ_C 153.1–153.4

ppm ([*mrm*], [*rrm*], [*rrr*], [*rmr*]) compares well with those reported in the literature for the atactic analogues.[21] The thermal properties of several copolymer samples (entries 2 and 10) were also examined by DSC analysis revealing the T_g values of 88.7 (Figgure S30) and 87.3 ^oC, respectively. These values are typical for such low molecular weight polymers falling in the regular range of those (45.0–118.9 ^oC) reported for polycarbonates.[22] No melting transitions were detected in these cases.

The fact that the experimentally determined by GPC average-number molecular weights, are systematically lower than the theoretical values, calculated from the initial monomer-to-initiator ratio and conversion values, are diagnostic of several possible phenomena operating under our conditions: initiation and growing of two polymer chains per one metal center, and occurrence of side transfer reactions, e.g. chain transfer to cyclohexane-1,2-diol generated from CHO in the presence of adventitious protic impurities (H_2O).[23] The latter phenomenon can also be responsible for the broadening of the molecular weight distributions of polymers obtained in the experiments carried out with low amounts of **1a-Y** (entry 12). In order to probe this hypothesis, copolymerization experiment with 2 equiv. of cyclohexane-1,2-diol was carried out (entry 13). Thus, the lower CHO conversion (60 %) was achieved as compared to that in the experiment without cyclohexane-1,2-diol (95% conversion, entry 5). The PDI value was found to be much broader (8.30 *vs* 1.99, respectively), which is diagnostic of poorly controlled transfer processes operating under these conditions and/or of multi-site behavior of the catalytic system.

Alkyl compounds of main-group metals are known not only to promote the copolymerization of CO_2 with epoxides,[24] but also to contribute to the formation of highly

active polynuclear systems derived from transition metals.[6d,e,g,h,19] The effect of the addition of such alkyl metal (Zn, Mg, Al) reagents to **1a-Y** was also investigated in copolymerization (entries 14–16) and, despite our expectations, appeared to be detrimental. The efficiency of the resulting binary systems was found to be much lower than that of the mono-component **1a-Y**.

Dinuclear alkyl group-free complexes [**1b-Sc]$_2$** and [**1b-Y]$_2$** were also probed as promoters of copolymerization (entries 17 and 18, respectively). Under identical conditions (70 °C, 18 h), only small amounts of polymers were isolated (14 and 31 % conversion, respectively), which were identified by NMR spectroscopy as polyethers (Figure S32),[7a] homopolymers of CHO. The different nature of initiating groups (alkyl vs phenolate group) may account for the reactivity and selectivity differences in these systems.[25] This observation also parallels the results reported by Chakraborty *et al.* for dinuclear titanium and zirconium complexes, which produced poly(cyclohexene oxide) polymers in the absence of a nucleophilic cocatalyst.[26]

CONCLUSIONS

In summary, we investigated complexation of two types of ligand platforms, namely, bis(imino)phenoxy and bis(amido)phenoxy, with group 3 metals. During this study, a series of new complexes of scandium and yttrium were obtained by σ-bond metathesis (alkane elimination) and completely characterized. Among them, bis(alkyl) complex $\{N^2O\}Y(CH_2SiMe_3)_2(THF)_2$ (**1a-Y**) was used for studies on stoichiometric C–H activation of 2-phenylpyridine selectively affording under mild conditions an original bis(aryl) product,

complex {N^{2}O}Y(η^2-*N*,C-2'-PhPy)$_2$(THF) (**3a-Y**). The latter was found stable in solution under ambient conditions and completely reluctant in reactions with weak electrophiles, such as styrene, imines and hydrosilanes. This reaction of formation of **3a-Y** from **1a-Y** and 2-phenylpyridine through a series of C–H activation steps was studied by DFT calculations, and the inactivity of **3a-Y** towards styrene was also rationalized. Attempts to use **1a-Y**, in combination with borane and borate activators for the hydroarylation of styrene and imines were also unsuccessful.

Gratifyingly, **1a-Y** found application as initiator of copolymerization of CO_2 with cyclohexene epoxide under mild conditions (70 °C, 12 bar of CO_2 pressure, toluene). The corresponding polycarbonate polymers were obtained with nearly quantitative conversion over 5 h of polymerization and high selectivity (97–99 % of carbonate units). Yet, this system constitutes a rare example of most efficient rare-earth metal alkyl complexes for copolymerization of CO_2 with epoxides (TON of 460) operating under mild conditions. These results again highlight the high potential of group 3 metal alkyl complexes in catalysis. Further studies of the development of new ligand platforms for C–H activation chemistry and CO_2 transformations are ongoing in our laboratories.

EXPERIMENTAL SECTION

General Considerations. All manipulations were performed under a purified argon atmosphere using standard Schlenk techniques or in a glovebox. Solvents were distilled from Na/benzophenone (THF, Et_2O) and Na/K alloy (toluene, pentane) under argon, degassed thoroughly, and stored under nitrogen prior to use. Deuterated solvents (benzene-d_6,

toluene-d_8, THF-d_8, >99.5 % D, Deutero GmbH and Euroisotop) were vacuum transferred from Na/K alloy into storage tubes. The ligand precursors **1a-H**,[8a] **1b-H$_3$**,[8b] Me_3SiCH_2Li,[27] $M(CH_2SiMe_3)_3(THF)_2$, $M(CH_2C_6H_4$-*o*-$NMe_2)_3$,[28] **CpSc^R**,[4a] **CpY^R** [4b] and **{N^4}M^R** [16] (M = Sc, Y) were prepared according to the published procedures. Styrene and cyclohexene oxide were distilled from CaH_2 and stored in the fridge at −25 °C. 2-Phenylpyridine, PhOMe, $PhNMe_2$, $PhSiH_3$, Et_3SiH were dried with 4Å molecular sieves and stored under argon. Other starting materials were purchased from Acros, Strem and Aldrich, and used as received.

Instruments and Measurements. NMR spectra of complexes were recorded on Bruker AM-400, and AM-500 spectrometers in Teflon-valved NMR tubes at 25 °C, unless otherwise indicated. ^1H, ^{13}C chemical shifts are reported in ppm *vs* $SiMe_4$ (0.00), as determined by reference to the residual solvent peaks. The resonances of organometallic complexes were assigned from 2D ^1H–^1H COSY, ^1H–^{13}C HSQC and HMBC NMR experiments. Coupling constants are given in hertz. Elemental analyses (C, H, N) were performed using a Flash EA1112 CHNS Thermo Electron apparatus and are the average of two independent determinations. DSC measurements were performed on a SETARAM Instrumentation DSC 131 differential scanning calorimeter at a heating rate of 10 °/min, first and second runs were recorded after cooling to 30 °C. Size exclusion chromatography (SEC) of polycarbonate samples was performed in THF (1 mL·min^{-1}) at 20 °C using a Polymer Laboratories PL50 apparatus equipped with PLgel 5 μm MIXED-C 300 × 7.5 mm columns, and combined RI and Dual angle LS (PL-LS 45/90°) detectors. The number average molecular weights (M_n) and polydispersities (Đ) of the polymers were calculated with reference to a universal calibration *vs*. polystyrene standards. The microstructure of polycarbonate was determined by

^{1}H and ^{13}C NMR spectroscopy according to the published procedures.[21] MALDI-TOF spectra were acquired on a Bruker Ultraflex-III TOF/TOF mass spectrometer (Bruker Daltonics, Inc., Billerica, MA) equipped with a Nd-YAG laser (355 nm). CH_3COONa was added for facilitating ion formation, and *trans*-2-[3-(4-*tert*-butylphenyl)-2-methyl-2-propenylidene]malononitrile was used as matrix.

Reaction between 1a-H and $Sc(CH_2SiMe_3)_3(THF)_2$. Formation of complex 1a-Sc. In the glovebox, in a Teflon-valved NMR tube was placed **1a-H** (0.026 g, 0.05 mmol), $Sc(CH_2SiMe_3)_3(THF)_2$ (0.023 g, 0.05 mmol). To this mixture, C_6D_6 (*ca*. 0.5 mL) was vacuum-transferred in at −25 °C and the tube was shaken for 1 h at room temperature. ^{1}H NMR spectroscopy indicated quantitative consumption of both reagents and formation of **1a-Sc** and **1a-Sc'** in ~1:0.3 ratio, respectively. Compound **1a-Sc** (some resonances couldn't be assigned unequivocally): ^{1}H NMR (500 MHz, C_6D_6, 25 °C): δ 9.20 (br s, 1H, C*H*=N), 9.00 (br s, 1H, Ar), 8.16 (br s, 1H, C*H*=N), 7.35 (br s, 1H, Ar), 3.89 (br m, 4H, α-CH_2, THF), 3.29 (br m, 4H, C*H*(CH_3)$_2$), 1.34 (m, 4H, β-CH_2, THF), 1.39–1.26 (m, 24H, CH(CH_3)$_2$), 1.21 (s, 9H, C(CH_3)$_3$), 0.08 (s, 18H, Si(CH_3)$_3$), –0.01 (s, 4H, ScCH_2). ^{13}C{^{1}H} NMR (125 MHz, C_6D_6, 25 °C): δ 172.4 (*C*H=N), 158.6 (*C*H=N), 150.9 (Ar), 148.9 (Ar), 140.9 (Ar), 137.4 (Ar), 135.2 (Ar), 131.6 (Ar), 127.1 (Ar), 124.1 (Ar), 122.9 (Ar), 122.3 (Ar), 68.6 (α-*C*H_2, THF), 40.4 (Sc*C*H_2), 28.6 (*C*H), 28.2 (*C*H), 28.1 (*C*H_3), 25.8 (*C*H_3), 25.0 (β-*C*H_2, THF), 23.1 (*C*H_3), 22.2 (*C*H_3), 3.3 (Si(*C*H_3)$_3$).

Compound 1a-Sc' (some resonances couldn't be assigned unequivocally): ^{1}H NMR (500 MHz, C_6D_6, 25 °C): δ 8.90 (d, ^4J = 2.6, 2H, Ar), 7.93 (s, 2H, C*H*=N), 7.45 (s, 2H, C*H*=N), 7.30–7.19 (m, 10H, Ar), 7.19 (d, ^4J = 2.6, 2H, Ar), 6.93 (d, J = 7.5, 2H, Ar), 6.82 (d,

J = 7.5, 2H, Ar), 6.57 (t, *J* = 7.5, 2H, Ar), 3.22 (q, *J* = 6.8, 2H, C*H*(C*H*$_3$)$_2$), 3.10 (q, *J* = 6.8, 4H, C*H*(C*H*$_3$)$_2$), 2.63 (q, *J* = 6.8, 2H, C*H*(C*H*$_3$)$_2$), 1.18 (s, 18H, C(C*H*$_3$)$_3$), 1.00–0.82 (m, 48H, CH(C*H*$_3$)$_2$), 0.67 (d, $^2J_{HH}$ = 12.7, 1H, ScC*H*$_2$), 0.08 (s, 18H, Si(C*H*$_3$)$_3$), –0.25 (d, $^2J_{HH}$ = 12.7, 1H, ScC*H*$_2$). ^{13}C{^{1}H} NMR (125 MHz, C_6D_6, 25 °C): δ 172.5 (*C*H=N), 164.2 (Ar), 164.1 (Ar), 156.8 (*C*H=N), 150.9 (Ar), 150.7 (Ar), 148.1 (Ar), 140.1 (Ar), 140.0 (Ar), 139.9 (Ar), 139.8 (Ar), 136.6 (Ar), 134.8 (Ar), 132.3 (Ar), 126.9 (Ar), 126.0 (Ar), 123.9 (Ar), 123.4 (Ar), 123.0 (Ar), 122.6 (Ar), 42.9 (Sc*C*H$_2$), 33.8 (*C*H), 30.8(*C*H), 29.8(*C*H), 28.1(*C*H), 25.1 (*C*H$_3$), 23.3 (*C*H$_3$), 22.4 (*C*H$_3$), 22.0 (*C*H$_3$), 21.9 (*C*H$_3$), –0.4 (Si(*C*H$_3$)$_3$).

All volatiles were removed in vacuum and hexane (1 mL) was added. Colorless crystals of **1a-Sc** (0.0070 g, 15 %), suitable for X-ray diffraction study, were isolated after the solution was kept for 7 days at –25 °C.

Synthesis of complex 1a-Y. A solution of **1a-H** (0.525 g, 1.0 mmol) in hexane (5.0 mL) was added quickly to a solution of Y(CH$_2$Si(CH$_3$)$_3$)$_3$(THF)$_2$ (0.495 g, 1.0 mmol) in hexane (5.0 mL) at –25 °C. The resulted reaction mixture was stirred at room temperature for 2 h. Green crystals of **1a-Y** were obtained (0.623 g, 67 %) after the solution was kept for 2 days at –25 °C. ^{1}H NMR (500 MHz, C_7D_8, 25 °C): δ 8.70–8.02 (br m, 4H, C*H*=N + Ar), 7.20–7.14 (m, 6H, Ar), 3.79 (s, 8H, α-C*H*$_2$, THF), 3.20 (br m, 4H, C*H*(C*H*$_3$)$_2$), 1.36–1.25 (m, 52H, β-C*H*$_2$ (THF) + CH(C*H*$_3$)$_2$ + C(C*H*$_3$)$_3$), 0.12 (s, 18H, Si(C*H*$_3$)$_3$), –0.71 (s, 4H, YC*H*$_2$). ^{13}C{^{1}H} NMR (125 MHz, C_7D_8, 25 °C) (many aromatic signals were not observed due to fluxional dynamics and overlapping): δ 165.4 (*C*=N), 151.0 (*C*=N), 139.1 (Ar), 133.9 (Ar), 123.6 (Ar), 70.4 (α-*C*H$_2$, THF), 34.1 (*C*HCH$_3$), 32.3 (br s, Y*C*H$_2$), 31.4 (*C*HCH$_3$), 28.6 (*C*H$_3$), 25.4 (*C*H$_3$), 23.9 (β-*C*H$_2$, THF), 4.4 (Si(*C*H$_3$)$_3$). Anal. Calcd for $C_{52}H_{85}N_2O_3Si_2Y$: C, 67.06;

H, 9.20; N, 3.01. Found: C, 67.30; H, 9.46; N, 2.92.

Reaction between 1b-H_3 and $Sc(CH_2SiMe_3)_3(THF)_2$. Formation of complex [1b-Sc]$_2$. Using a similar procedure, described for **1a-Y**, complex **[1b-Sc]$_2$** was prepared from **1b-H_3** (0.0528 g, 0.1 mmol) and $Sc(CH_2SiMe_3)_3(THF)_2$ (0.0450 g, 0.1 mmol). Colorless crystals of **[1b-Sc]$_2$** (0.029 g, 45 %) were obtained after the solution was kept for 3 days at –25 °C. ^{1}H NMR (500 MHz, C_6D_6, 25 °C): δ 7.39 (br m, 6H, Ar), 7.32–6.74 (br m, 8H, Ar), 6.74 (br m, 2H, Ar), 5.60 (br m, 2H, CH_2N), 5.29 (br m, 2H, CH_2N), 4.41 (br m, 2H, CH(CH_3)$_2$), 4.06 (br m, 2H, CH_2N), 4.00 (br m, 4H, α-CH_2, THF), 3.85 (br m, 2H, CH_2N), 3.53 (br m, 6H, α-CH_2, THF + CH(CH_3)$_2$), 2.97 (br m, 4H, CH(CH_3)$_2$), 1.77 (br m, 6H, C(CH_3)$_3$), 1.60–0.70 (br m, 62H, CH(CH_3)$_2$ + β-CH_2 (THF) + C(CH_3)$_3$), 0.43 (br m, 6H, C(CH_3)$_3$) . ^{13}C{^{1}H} NMR (125 MHz, C_6D_6, 25 °C) (due to a strong fluxional dynamics some of the aromatic signals could not be observed): δ 153.7 (Ar), 152.2 (Ar), 145.3 (Ar), 123.6 (Ar), 71.6 (α-CH$_2$, THF), 62.8 (CH$_2$N), 55.8 (CH$_2$N), 31.1 (CHCH$_3$), 29.3 (CHCH$_3$), 28.1 (CH$_3$), 26.8 (CH$_3$), 23.8 (β-CH$_2$, THF), 22.6 (CH$_3$). Anal. Calcd for $C_{72}H_{98}N_4O_2Sc_2$: C, 75.76; H, 8.65; N, 4.91. Found C, 75.84; H, 8.69; N, 4.73.

Reaction between 1b-H_3 and $Y(CH_2SiMe_3)_3(THF)_2$. Formation of complex [1b-Y]$_2$. Using a similar procedure, described for **1a-Y**, complex **[1b-Y]$_2$** was prepared from **1b-H_3** (0.053 g, 0.1 mmol) and $Y(CH_2Si(CH_3)_3)_3(THF)_2$ (0.050 g, 0.1 mmol). Yellow crystals of **[1b-Y]$_2$** (0.024 g, 39 %) were obtained after the solution was kept for 7 days at −25 °C. ^{1}H NMR (500 MHz, toluene-d_8, 25 °C): δ 7.20−6.96 (m, 16H, Ar), 5.25 (d, $^2J_{HH}$ = 14.6, 4H, CH_2N), 3.95 (d, $^2J_{HH}$ = 14.6, 4H, CH_2N), 3.80–3.00 (br m, 16H, α-CH_2, THF + CH(CH_3)$_2$), 1.34−1.11 (m, 74H, β-CH_2 (THF) + CH(CH_3)$_2$ + C(CH_3)$_3$). ^{13}C{^{1}H} NMR (125 MHz,

toluene-d_8, 25 °C): δ 152.5 (Ar), 145.2 (Ar), 131.8 (Ar), 128.1 (Ar), 127.8 (Ar), 127.2 (Ar), 125.3 (Ar), 124.3 (Ar), 123.4 (Ar), 122.6 (Ar), 70.7 (α-CH_2, THF), 62.6 (*C*H_2N), 59.5 (*C*H_2N), 33.5 (*C*HCH$_3$), 31.6 (*C*HCH$_3$), 31.3 (*C*HCH$_3$), 28.2 (*C*H$_3$), 25.2 (β-CH_2, THF), 24.9 (*C*H$_3$), 22.8 (*C*H$_3$). Anal. Calcd for $C_{72}H_{98}N_4O_2Y_2$: C, 70.34; H, 8.04; N, 4.56. Found C, 70.05; H, 8.40; N, 4.03.

Synthesis of complex 3a-Y. To a solution of **1a-Y** (0.0930 g, 0.10 mmol) in hexane (2.0 mL) was added 2-phenylpyridine (28.4 μL, 0.20 mmol) in hexane (1.0 mL) at –25 °C. The solution was stirred at room temperature for 3 h. Dark green crystals of **3a-Y** (0.053 g, 54 %) were obtained after the solution was kept for 7 days at –25 °C. ^{1}H NMR (500 MHz, toluene-d_8, 25 °C): δ 8.74 (br m, 2H, C*H*=N), 8.57 (d, *J* = 4.8, 1H, Ar), 8.46 (d, *J* = 4.8, 2H, PhPy), 8.11 (d, 2H, *J* = 7.6, PhPy), 7.81 (br m, 2H, PhPy), 7.61 (d, 2H, *J* = 4.8, PhPy), 7.45 (d, 2H, *J* = 7.8, PhPy), 7.27 (m, 3H, Ar), 7.20 (d, 1H, *J* = 8.0, Ar), 7.18−7.12 (m, 4H, Ar), 6.95 (t, 3H, *J* = 7.6, PhPy), 6.70 (dd, *J* = 4.8, 7.6, 1H, Ar), 6.23 (t, *J* = 6.2, 2H, PhPy), 3.42 (br m, 4H, α-CH_2, THF), 3.14 (br m, 4H, C*H*(CH$_3$)$_2$), 1.43−1.10 (m, 16H, β-CH_2 (THF) + CH(CH_3)$_2$), 0.94−0.87 (m, 9H, C(CH_3)$_3$). ^{13}C{^{1}H} NMR (125 MHz, toluene-d_8, 25 °C) (some of the quaternary aromatic signals could not be observed): δ 190.8 (d, $^1J_{Y\text{-}C}$ = 41.6, Y-*C*(PhPy)), 166.6 (*C*=NH), 165.7 (PhPy), 157.1 (*C*=NH), 149.5 (PhPy), 149.2 (PhPy), 145.7 (PhPy), 139.6 (Ar), 139.6 (PhPy), 138.2 (Ar), 137.8 (Ar), 137.4 (Ar), 135.8 (Ar), 129.9 (PhPy), 128.8 (Ar), 128.2 (Ar), 126.8 (Ar), 124.5 (Ar), 123.1 (PhPy), 121.5 (Ar), 119.5 (Ar), 118.6 (PhPy), 68.5 (α-CH_2, THF), 33.7 (*C*H(CH$_3$)$_2$), 31.6 (*C*H$_3$), 31.1 (*C*(CH$_3$)), 28.4 (*C*H$_3$), 24.8 (CH(*C*H$_3$)$_2$), 23.5–22.7 (br m, β-CH_2 (THF) + *C*H(CH$_3$)$_2$ + C(*C*H$_3$)). Anal. Calcd for $C_{62}H_{70}N_4O_2Y$: C, 75.06; H, 7.11; N, 5.65. Found C, 75.18; H, 7.39; N, 5.77.

Crystal Structure Determination of Complexes 1a-M, 2a-M, [1b-M]$_2$ and 3a-Y (M = Sc and Y). Diffraction data were collected at 150(2) K using a Bruker APEX CCD diffractometer with graphite-monochromatized Mo-Kα radiation (λ = 0.71073 Å). The crystal structures were solved by direct methods, remaining atoms were located from difference Fourier synthesis followed by full-matrix least-squares refinement based on F2 (programs SIR97 and SHELXL-97).[29] Many hydrogen atoms could be located from the Fourier difference analysis. Other hydrogen atoms were placed at calculated positions and forced to ride on the attached atom. The hydrogen atom positions were calculated but not refined. All non-hydrogen atoms were refined with anisotropic displacement parameters. Crystal data and details of data collection and structure refinement for the different compounds are given in Table S1. Crystal data, details of data collection and structure refinement for all compounds (CCDC 2016816–2016822, respectively) can be obtained from the Cambridge Crystallographic Data Centre via www.ccdc.cam.ac.uk/data_request/cif.

Computational Studies. The calculations were performed using the Gaussian 09[30] program employing B3PW91[31] functional, and using a standard double-ξ polarized basis set, namely the LANL2DZ set, augmented with a single polarization *f* function on yttrium (0.835) and a single polarization *d* function on silicon (0.296). The solvent effects, in our case for toluene, were taken into account during all the calculations by means of the SMD model.[32] All stationary points were fully characterized via analytical frequency calculations as either true minima (all positive eigenvalues) or transition states (one imaginary eigenvalue). The IRC procedure was used to confirm the nature of each transition state connecting two minima.[33] Zero-point vibrational energy corrections (ZPVE) were estimated by a frequency

calculation at the same level of theory, to be considered for the calculation of the total energy values at $T = 298$ K in the same way as in the approach used by Castro et *al*.[34]

Typical procedure for hydroarylation of styrene with 2-phenyl-pyridine in the presence of group 3 metal complexes. In a typical experiment (Table S1, entry 4), in the glovebox, to a Teflon-valved NMR tube was placed **1a-Y** (0.0093 g, 0.01 mmol), 2-phenylpyridine (14.20 μL, 0.10 mmol), styrene (11.50 μL, 0.10 mmol), and C_6D_6 (0.5 mL) was added at –25 °C. The tube was sealed at room temperature and the mixture was heated at the required temperature for the desired time. Progress of the reaction was monitored by ^{1}H NMR spectroscopy.

Typical Procedure for Copolymerization of CO_2 with CHO. In a typical experiment (Table 1, entry 5), in the glovebox, a Schlenk tube was charged with CHO (1.0 mL, 9.9 mmol), **1a-Y** (0.02 g, 0.05 mmol) and toluene (1.0 mL). The mixture was transferred to an autoclave equipped with a magnetic stirring bar under argon and, then, pressurized at CO_2 (12 bar). The reaction mixture was stirred vigorously at the required temperature for the desired time. After cooling to room temperature, CO_2 was released and a small amount of the resulting mixture was analyzed by ^{1}H NMR spectroscopy to determine the conversion and selectivity. The reaction mixture was quenched by the addition of MeOH/HCl, then poured into a large amount of MeOH to precipitate the polymer, which was dried under vacuum at 40 °C and weighted.

ASSOCIATED CONTENT

Supporting Information. Crystallographic data; representative NMR and MALDI-TOF

spectra of complexes and polymers; DSC curves; DFT computations.

ACKNOWLEDGEMENTS

The authors are grateful to the PHC Cai Yuanpei program between Campus France and Chinese Research Council. EK thanks ENSCR and the CTI group of ISCR for computational facilities, and acknowledges support from ANR-17-CE06-0006-01 "CO22CHEM". We are grateful to Dr Vincent Dorcet (Univ Rennes) for resolving the structure of **1a-Y** and to Lihua Hu (Soochow University) for MALDI-ToF analyses.

REFERENCES

1 a) D. C. Bradley, R. M. Mehrotra, I. P. Rothwell, A. Singh, *Alkoxo and Aryloxo Derivatives of Metals*, Academic Press, London, 2001; b) The Chemistry of Metal Phenolates *in* PATAI'S Chemistry of Functional Groups, (Ed. Zabicky, J.), John Wiley & Sons, Ltd, 2014.

2 Edelmann, F. T.; Freckmann, D. M. M.; Schumann, H. Synthesis and Structural Chemistry of Non-Cyclopentadienyl Organolanthanide Complexes. *Chem. Rev.* **2002**, *102*, 1851–1896.

3 Arnold, P. L.; McMullon, M. W.; Rieb, J.; Kuhn, F. E. C–H Bond Activation by *f*-Block Complexes. *Angew. Chem. Int. Ed.* **2015**, *54*, 82–100.

4 For recent articles, see: (a) Guan, B.-T.; Hou, Z. Rare-Earth-Catalyzed C–H Bond Addition of Pyridines to Olefins. *J. Am. Chem. Soc.* **2011**, *133*, 18086–18089; (b) Oyamada, J.; Hou, Z. Regioselective C–H Alkylation of Anisoles with Olefins

Catalyzed by Cationic Half-Sandwich Rare Earth Alkyl Complexes. *Angew. Chem. Int. Ed.* **2012**, *51*, 12828–12832; (c) Guan, B.-T.; Wang, B.; Nishiura, M.; Hou, Z. Yttrium-Catalyzed Addition of Benzylic C–H Bonds of Alkyl Pyridines to Olefins. *Angew. Chem. Int. Ed.* **2013**, *52*, 4418–4421; (d) Song, G.; Luo, G.; Oyamada, J.; Luo, Y.; Hou, Z. Ortho-Selective C–H Addition of *N,N*-Dimethyl Anilines to Alkenes by a Yttrium Catalyst. *Chem. Sci.* **2016**, *7*, 5265–5270; (e) Nako, A. E.; Oyamada, J.; Nishiura, M.; Hou, Z. Scandium-Catalysed Intermolecular Hydroaminoalkylation of Olefins with Aliphatic Tertiary Amines. *Chem. Sci.* **2016**, *7*, 6429–6434; (f) Nagae, H.; Shibata, Y.; Tsurugi, H.; Mashima, K. Aminomethylation Reaction of ortho-Pyridyl C–H Bonds Catalyzed by Group 3 Metal Triamido Complexes. *J. Am. Chem. Soc.* **2015**, *137*, 640–643; (g) Kundu, A.; Inoue, M.; Nagae, H.; Tsurugi, H.; Mashima, K. Direct Ortho-C-H Aminoalkylation of 2-Substituted Pyridine Derivatives Catalyzed by Yttrium Complexes with *N,N′*-Diarylethylenediamido Ligands. *J. Am. Chem. Soc.* **2018**, *140*, 7332–7342.

5 See some recent reviews: (a) Guillaume, S. M. Recent Advances in Ring-Opening Polymerization Strategies toward α,ω-Hydroxy Telechelic Polyesters and Resulting Copolymers. *Eur. Polym. J.* **2013**, *49*, 768–779; (b) Trifonov, A. A.; Lyubov, D. M. A Quarter-Century Long Story of Bis (Alkyl) Rare-Earth (III) Complexes. *Coord. Chem. Rev.* **2017**, *340*, 10–61; (c) Lyubov, D. M.; Tolpygin, A. O.; Trifonov, A. A. Rare-Earth Metal Complexes as Catalysts for Ring-Opening Polymerization of Cyclic Esters. *Coord. Chem. Rev.* **2019**, *392*, 83–145.

6 See some recent reviews: (a) Coates, G. W.; Moore, D. R. Discrete Metal-Based

Catalysts for the Copolymerization of CO_2 and Epoxides: Discovery, Reactivity, Optimization, and Mechanism. *Angew. Chem. Int. Ed.* **2004**, *43*, 6618–6639; (b) Klaus, S.; Lehenmeier, M. W.; Anderson, C. E.; Rieger, B. Recent Advances in CO_2/Epoxide Copolymerization-New Strategies and Cooperative Mechanisms. *Coord. Chem. Rev.* **2011**, *255*, 1460–1479; (c) Kember, M. R.; Buchard, A.; Williams, C. K. Catalysts for CO_2/Epoxide Copolymerisation. *Chem. Commun.* **2011**, *47*, 141–163; (d) Taherimehr, M.; Pescarmona, P. P. Green Polycarbonates Prepared by the Copolymerization of CO_2 with Epoxides. *J. Appl. Polym. Sci.* **2014**, *131*, 1–17; (e) Poland, S. J.; Darensbourg, D. J. A Quest for Polycarbonates Provided: Via Sustainable Epoxide/CO_2 Copolymerization Processes. *Green Chem.* **2017**, *19*, 4990–5011; (f) Kozak, C. M.; Ambrose, K.; Anderson, T. S. Copolymerization of Carbon Dioxide and Epoxides by Metal Coordination Complexes. *Coord. Chem. Rev.* **2018**, *376*, 565–587; (g) Scharfenberg, M.; Hilf, J.; Frey, H. Functional Polycarbonates from Carbon Dioxide and Tailored Epoxide Monomers: Degradable Materials and Their Application Potential. *Adv. Funct. Mater.* **2018**, *28*, 1–16; (h) Kamphuis, A. J.; Picchioni, F.; Pescarmona, P. P. CO_2-Fixation into Cyclic and Polymeric Carbonates: Principles and Applications. *Green Chem.* **2019**, *21*, 406–448.

7 For recent articles, see: (a) Cui, D.; Nishiura, M.; Hou, Z. Alternating Copolymerization of Cyclohexene Oxide and Carbon Dioxide Catalyzed by Organo Rare Earth Metal Complexes. *Macromolecules* **2005**, *38*, 4089–4095; (b) Zhang, Z.; Cui, D.; Liu, X. Alternating Copolymerization of Cyclohexene Oxide and Carbon Dioxide Catalyzed by Noncyclopentadienyl Rare-Earth Metal Bis(Alkyl) Complexes. *J. Polym. Sci. Pol.*

Chem. **2008**, *46*, 6810–6818; (c) Decortes, A.; Haak, R. M.; Martín, C.; Belmonte, M. M.; Martin, E.; Benet-Buchholz, J.; Kleij, A. W. Copolymerization of CO_2 and Cyclohexene Oxide Mediated by Yb(Salen)-Based Complexes. *Macromolecules* **2015**, *48*, 8197–8207; (d) Qin, J.; Xu, B.; Zhang, Y.; Yuan, D.; Yao, Y. Cooperative Rare Earth Metal-Zinc Based Heterometallic Catalysts for Copolymerization of CO_2 and Cyclohexene Oxide. *Green Chem.* **2016**, *18*, 4270–4275; (e) Hua, L.; Li, B.; Han, C.; Gao, P.; Wang, Y.; Yuan, D.; Yao, Y. Synthesis of Homo- and Heteronuclear Rare-Earth Metal Complexes Stabilized by Ethanolamine-Bridged Bis(Phenolato) Ligands and Their Application in Catalyzing Reactions of CO_2 and Epoxides. *Inorg. Chem.* **2019**, *58*, 8775–8786; (f) Ho, C. H.; Chuang, H. J.; Lin, P. H.; Ko, B. T. Copolymerization of Carbon Dioxide with Cyclohexene Oxide Catalyzed by Bimetallic Dysprosium Complexes Containing Hydrazine-Functionalized Schiff-Base Derivatives. *J. Polym. Sci. Pol. Chem.* **2017**, *55*, 321–328; (g) Xu, R.; Hua, L.; Li, X.; Yao, Y.; Leng, X.; Chen, Y. Rare-Earth/Zinc Heterometallic Complexes Containing Both Alkoxy-Amino-Bis(Phenolato) and Chiral Salen Ligands: Synthesis and Catalytic Application for Copolymerization of CO_2 with Cyclohexene Oxide. *Dalton Trans.* **2019**, *48*, 10565–10573; (h) Nagae, H.; Aoki, R.; Akutagawa, S.; Kleemann, J.; Tagawa, R.; Schindler, T.; Choi, G.; Spaniol, T. P.; Tsurugi, H.; Okuda, J.; Mashima, K. Lanthanide Complexes Supported by a Trizinc Crown Ether as Catalysts for Alternating Copolymerization of Epoxide and CO_2: Telomerization Controlled by Carboxylate Anions. *Angew. Chem. Int. Ed.* **2018**, *57*, 2492–2496.

8 (a) Wang, L.; Sun, W.; Han, L.; Li, Z.; Hu, Y.; He, C.; Yan, C. Cobalt and Nickel Complexes Bearing 2,6-Bis(imino)phenoxy Ligands: Syntheses, Structures and Oligomerization Studies. *J. Organomet. Chem.* **2002**, *650*, 59–64; (b) Hu, Q.; Jie, S.; Braunstein, P.; Li, B.-G. Highly Active Tridentate Amino-phenol Zinc Complexes for the Catalytic Ring-opening Polymerization of ε-Caprolactone. *J. Organomet. Chem.* **2019**, *882*, 1–9.

9 Emslie, D. J. H.; Piers, W. E.; Parvez, M.; McDonald, R. Organometallic Complexes of Scandium and Yttrium Supported by a Bulky Salicylaldimine Ligand. *Organometallics* **2002**, *21*, 4226–4240.

10 For the structurally close complexes $\{\eta^2$-1-[CH=N-Ar]-2-O-3-*t*Bu-$C_6H_3\}Y(CH_2SiMe_3)_2(THF)_n$ (n = 1 and 2 (**I-Y**)), a fluxional dynamic process was explained by a reversible decoordination of THF molecule and interconversion between isomers arising from the relative positioning of the two alkyl groups around the metal center, see ref.[9].

11 Effective ionic radii for 6-coordinate centers: Sc^{3+}, 0.745 Å; Y^{3+}, 0.900 Å. Shannon, R. D. Revised effective ionic radii and systematic studies of interatomic distances in halides and chalcogenides. *Acta Cryst.* **1976**, *A32*, 751–767.

12 Duan, Y.-L.; He, J.-X.; Wang, W.; Zhou, J.-J.; Huang, Y.; Yang, Y. Synthesis and Characterization of Dinuclear Rare-Earth Complexes Supported by Amine-Bridged Bis(Phenolate) Ligands and Their Catalytic Activity for the Ring-Opening Polymerization of $_L$-Lactide. *Dalton Trans.* **2016**, *45*, 10807–10820.

13 (a) Carver, C. T.; Diaconescu, P. L. Ring-Opening Reactions of Aromatic

N-Heterocycles by Scandium and Yttrium Alkyl Complexes. *J. Am. Chem. Soc.* **2008**, *130*, 7558–7559; (b) Carver, C. T.; Benitez, D.; Miller, K. L.; Williams, B. N.; Tkatchouk, E.; Gooddard III, W. A.; Diaconescu, P. L. Reactions of Group III Biheterocyclic Complexes. *J. Am. Chem. Soc.* **2009**, *131*, 10269–10278; (c) Williams, B. N.; Huang, W.; Miller, K. L.; Diaconescu, P. L. Group 3 Metal Complexes of Radical-Anionic 2,2′-Bipyridyl Ligands. *Inorg. Chem.* **2010**, *49*, 11493–11498. (d) Williams, B. N.; Benitez, D.; Miller, K. L.; Tkatchouk, E.; Goddard III, W. A.; Diaconescu, P. L. An Unusual Hydrogen Migration/C–H Activation Reaction with Group 3 Metals. *J. Am. Chem. Soc.* **2011**, *133*, 4680–4683.

14 (a) Kaneko, H.; Nagae, H.; Tsurugi, H.; Mashima, K. End-Functionalized Polymerization of 2-Vinylpyridine through Initial C–H Bond Activation of *N*-Heteroaromatics and Internal Alkynes by Yttrium Ene-Diamido Complexes. *J. Am. Chem. Soc.* **2011**, *133*, 19626–19629; (b) Shibata, Y.; Nagae, H.; Sumiya, S.; Rochat, R.; Tsurugi, H.; Mashima, K. 2,2'-Bipyridyl Formation from 2-Arylpyridines through Bimetallic Diyttrium Intermediate. *Chem. Sci.* **2015**, *6*, 5394–5399.

15 (a) Zhu, X.; Li, Y.; Guo, D.; Wang, S.; Wei, Y.; Zhou, S. Versatile Reactivities of Rare-Earth Metal Dialkyl Complexes Supported by a Neutral Pyrrolyl-Functionalized β-Diketiminato Ligand. *Dalton Trans.* **2018**, *47*, 3947–3957; (b) Zhang, Y.; Zhang, J.; Hong, J.; Zhang, F.; Weng, L.; Zhou, X. Versatile Reactivity of β-Diketiminato-Supported Yttrium Dialkyl Complex toward Aromatic N-Heterocycles. *Organometallics* **2014**, *33*, 7052–7058.

16 Radkov, V.; Roisnel, T.; Trifonov, A.; Carpentier, J.-F.; Kirillov, E. Neutral and Cationic Alkyl and Amido Group 3 Metal Complexes of Amidine-Amidopyridinate Ligands: Synthesis, Structure and Polymerization Catalytic Activity. *Eur. J. Inorg. Chem.* **2014**, *25*, 4168–4178.

17 Cheng, M.; Moore, D. R.; Reczek, J. J.; Chamberlain, B. M.; Lobkovsky, E. B.; Coates, G. W. Single-Site β-Diiminate Zinc Catalysts for the Alternating Copolymerization of CO_2 and Epoxides: Catalyst Synthesis and Unprecedented Polymerization Activity. *J. Am. Chem. Soc.* **2001**, *123*, 8738–8749.

18 Moore, D. R.; Cheng, M.; Lobkovsky, E. B.; Coates, G. W. Mechanism of the Alternating Copolymerization of Epoxides and CO_2 Using β-Diiminate Zinc Catalysts: Evidence for a Bimetallic Epoxide Enchainment. *J. Am. Chem. Soc.* **2003**, *125*, 11911–11924.

19 (a) Ren, W. M.; Zhang, X.; Liu, Y.; Li, J. F.; Wang, H.; Lu, X. B. Highly Active, Bifunctional Co(III)-Salen Catalyst for Alternating Copolymerization of CO_2 with Cyclohexene Oxide and Terpolymerization with Aliphatic Epoxides. *Macromolecules* **2010**, *43*, 1396–1402; (b) Kissling, S.; Lehenmeier, M. W.; Altenbuchner, P. T.; Kronast, A.; Reiter, M.; Deglmann, P.; Seemann, U. B.; Rieger, B. Dinuclear Zinc Catalysts with Unprecedented Activities for the Copolymerization of Cyclohexene Oxide and CO_2. *Chem. Commun.* **2015**, *51*, 4579–4582; (c) Nagae, H.; Aoki, R.; Akutagawa, S. N.; Kleemann, J.; Tagawa, R.; Schindler, T.; Choi, G.; Spaniol, T. P.; Tsurugi, H.; Okuda, J.; Mashima, K. Lanthanide Complexes Supported by a Trizinc Crown Ether as Catalysts for Alternating Copolymerization of Epoxide and CO_2:

Telomerization Controlled by Carboxylate Anions. *Angew. Chem. Int. Ed.* **2018**, *57*, 2492–2496. (d) Deng, J.; Ratanasak, M.; Sako, Y.; Tokuda, H.; Maeda, C.; Hasegawa, J. Y.; Nozaki, K.; Ema, T. Aluminum Porphyrins with Quaternary Ammonium Halides as Catalysts for Copolymerization of Cyclohexene Oxide and CO_2: Metal-Ligand Cooperative Catalysis. *Chem. Sci.* **2020**, *11*, 5669–5675; (e) Deacy, A. C.; Kilpatrick, A. F. R.; Regoutz, A.; Williams, C. K. Understanding Metal Synergy in Heterodinuclear Catalysts for the Copolymerization of CO_2 and Epoxides. *Nat. Chem.* **2020**, *12*, 372–380.

20 Thevenon, A.; Cyriac, A.; Myers, D.; White, A. J. P.; Durr, C. B.; Williams, C. K. Indium Catalysts for Low-Pressure CO_2/Epoxide Ring-Opening Copolymerization: Evidence for a Mononuclear Mechanism? *J. Am. Chem. Soc.* **2018**, *140*, 6893–6903.

21 Nakano, K.; Nozaki, K.; Hiyama, T. Spectral Assignment of Poly[Cyclohexene Oxide-Alt-Carbon Dioxide]. *Macromolecules* **2001**, *34*, 6325–6332.

22 (a) Lee, I. K.; Ha, J. Y.; Cao, C.; Park, D. -W.; Ha, C. -S.; Kim, I. Effect of Complexing Agents of Double Metal Cyanide Catalyst on the Copolymerizations of Cyclohexene Oxide and Carbon Dioxide. *Catal. Today* **2009**, *148*, 389–397; (b) Meng, Q. Y.; Pepper, K.; Cheng, R. H.; Howdle, S. M.; Liu, B. P. Effect of Supercritical CO_2 on the Copolymerization Behavior of Cyclohexene Oxide/CO_2 and Copolymer Properties with DMC/Salen-Co(III) Catalyst System. *J. Polym. Sci. Pol. Chem.* **2016**, *54*, 2785–2793; (c) Mandal, M.; Chakraborty, D. Group 4 Complexes Bearing Bis(Salphen) Ligands: Synthesis, Characterization, and Polymerization Studies. *J. Polym. Sci. Pol. Chem.* **2016**, *54*, 809–824; (d) Nakano, K.; Nakamura, M.; Nozaki, K. Alternating

Copolymerization of Cyclohexene Oxide with Carbon Dioxide Catalyzed by (Salalen)CrCl Complexes. *Macromolecules* **2009**, *42*, 6972–6980.

23 (a) Kember, M. R.; Williams, C. K. Efficient Magnesium Catalysts for the Copolymerization of Epoxides and CO 2; Using Water to Synthesize Polycarbonate Polyols. *J. Am. Chem. Soc.* **2012**, *134*, 15676–15679; (b) Nakano, K.; Nakamura, M.; Nozaki, K. Alternating Copolymerization of Cyclohexene Oxide with Carbon Dioxide Catalyzed by (Salalen)CrCl Complexes. *Macromolecules* **2009**, *42*, 6972–6980; (c) Wu, G. P.; Darensbourg, D. J. Mechanistic Insights into Water-Mediated Tandem Catalysis of Metal-Coordination CO2/Epoxide Copolymerization and Organocatalytic Ring-Opening Polymerization: One-Pot, Two Steps, and Three Catalysis Cycles for Triblock Copolymers Synthesis. *Macromolecules* **2016**, *49*, 807–814; (d) Darensbourg, D. J. Chain Transfer Agents Utilized in Epoxide and CO_2 Copolymerization Processes. *Green Chem.* **2019**, *21*, 2214–2223.

24 (a) Inoue, S.; Koinuma, H.; Tsuruta, T. Copolymerization of Carbon Dioxide and Epoxide with Organometallic Compounds. *Die Makromol. Chemie* **1969**, *130*, 210–220; (b) Zhang, D.; Zhang, H.; Hadjichristidis, N.; Gnanou, Y.; Feng, X. Lithium-Assisted Copolymerization of CO_2/Cyclohexene Oxide: A Novel and Straightforward Route to Polycarbonates and Related Block Copolymers. *Macromolecules* **2016**, *49*, 2484–2492; (c) Ghosh, S.; Pahovnik, D.; Kragl, U.; Mejía, E. Isospecific Copolymerization of Cyclohexene Oxide and Carbon Dioxide Catalyzed by Dialkylmagnesium Compounds. *Macromolecules* **2018**, *51*, 846–852.

25 (a) Nicolás, S.; Itziar, R.; Soledad Larrechi, M.; Angels, S.; Ana, M. Spectroscopic

Evidence of the Mechanism Involved in the Cationic Diglycidyl Ether of Bisphenol a Curing with Rare Earth Metal Triflates. *Appl. Spectrosc.* **2010**, *64*, 104–111; (b) Liu, Y.; Yu, H. Y.; Lu, X. B. Fast Ring-Opening Polymerization of 1,2-Disubstituted Epoxides Initiated by a CoIII-Salen Complex. *Macromol. Chem. Phys.* **2019**, *220*, 1900377.

26 Mandal, M.; Monkowius, U.; Chakraborty, D. Synthesis and Structural Characterization of Titanium and Zirconium Complexes Containing Half-Salen Ligands as Catalysts for Polymerization Reactions. *New J. Chem.* **2016**, *40*, 9824–9839.

27 Lewis, H. L.; Brown, T. L. Association of Alkyllithium Compounds in Hydrocarbon Media. Alkyllithium-Base Interactions. *J. Am. Chem. Soc.* **1970**, *92*, 4664–4670.

28 Hultzsch, K. C.; Voth, P.; Beckerle, L.; Spaniol, T. P.; Okuda, J. Single-Component Polymerization Catalysts for Ethylene and Styrene: Synthesis, Characterization, and Reactivity of Alkyl and Hydrido Yttrium Complexes Containing a Linked Amido−Cyclopentadienyl Ligand. *Organometallics*, **2000**, *19*, 228−243.

29 (a) Sheldrick, G. M. SHELXS-97, Program for the Determination of Crystal Structures, University of Goettingen (Germany), 1997; (b) Sheldrick, G. M. SHELXL-97, Program for the Refinement of Crystal Structures, University of Goettingen (Germany), 1997. (c) Sheldrick, G. M. *Acta. Cryst.* **2008**, *A64*, 112.

30 Frisch, M. J.; Trucks, G. W.; Schlegel, H. B.; Scuseria, G. E.; Robb, M. A.; Cheeseman, J. R.; Scalmani, G.; Barone, V.; Mennucci, B.; Petersson, G. A.; Nakatsuji, H.; Caricato, M.; Li, X.; Hratchian, H. P.; Izmaylov, A. F.; Bloino, J.; Zheng, G.; Sonnenberg, J. L.; Hada, M.; Ehara, M.; Toyota, K.; Fukuda, R.;

Hasegawa, J.; Ishida, M.; Nakajima, T.; Honda, Y.; Kitao, O.; Nakai, H.; Vreven, T.; Montgomery, J. A., Jr.; Peralta, J. E.; Ogliaro, F.; Bearpark, M.; Heyd, J. J.; Brothers, E.; Kudin, K. N.; Staroverov, V. N.; Kobayashi, R.; Normand, J.; Raghavachari, K.; Rendell, A.; Burant, J. C.; Iyengar, S. S.; Tomasi, J.; Cossi, M.; Rega, N.; Millam, J. M.; Klene, M.; Knox, J. E.; Cross, J. B.; Bakken, V.; Adamo, C.; Jaramillo, J.; Gomperts, R.; Stratmann, R. E.; Yazyev, O.; Austin, A. J.; Cammi, R.; Pomelli, C.; Ochterski, J. W.; Martin, R. L.; Morokuma, K.; Zakrzewski, V. G.; Voth, G. A.; Salvador, P.; Dannenberg, J. J.; Dapprich, S.; Daniels, A. D.; Farkas, Ö.; Foresman, J. B.; Ortiz, J. V.; Cioslowski, J.; Fox, D. J. Gaussian 09, Revision D.01; Gaussian Inc.: Pittsburgh, PA, 2009.

31 (a) Becke, A. D. Density-Functional Exchange-Energy Approximation with Correct Asymptotic Behavior. *Phys. Rev. A* **1988**, *38*, 3098–3100. (b) Becke, A. D. Density-functional thermochemistry. III. The role of exact exchange. *J. Chem. Phys.* **1993**, *98*, 5648–5652.

32 Marenich, A. V.; Cramer, C. J.; Truhlar, D. G. Universal Solvation Model Based on Solute Electron Density and on a Continuum Model of the Solvent Defined by the Bulk Dielectric Constant and Atomic Surface Tensions. *J. Phys. Chem. B*, **2009**, *113*, 6378–6396.

33 Gonzales, C.; Schlegel, H. B. An Improved Algorithm for Reaction Path Following. *J. Chem. Phys.* **1989**, *90*, 2154–2161.

34 Castro, L.; Kirillov, E.; Miserque, O.; Welle, A.; Haspeslagh, L.; Carpentier, J.-F.; Maron, L. Are Solvent and Dispersion Effects Crucial in Olefin Polymerization DFT

Calculations? Some Insights from Propylene Coordination and Insertion Reactions with Group 3 and 4 Metallocenes. *ACS Catal.* **2015**, *5*, 416–425.

For Table of Contents Only

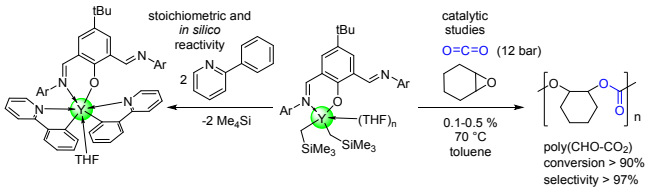

Synopsis

Mono and dinuclear group 3 metal complexes incorporating polydentate bis(imino)phenoxy $\{N^2O\}^-$ and bis(amido)phenoxy $\{N^2O\}^{3-}$ ligands were synthesized. Bis(alkyl) complex of yttrium was used for copolymerization of cyclohexene oxide with CO_2 giving polycarbonates with high efficiency and selectivity, and also for the selective C–H activation of 2-phenylpyridine affording the corresponding bis(aryl) product. The mechanism of the latter reaction was rationalized by DFT computations.